DRAFT Citation:
International Review of Electrical Engineering, 9(5), pp.1060-1070, 2014

Leading Edge Detection of RF-Signal for Power Arcing Source Location

Frank ZokoBle[1], MattiLehtonen[2], Ari Sihvola[3], Charles Kim[4]

Abstract – *Accurate power arc location can be realized via wideband signals emitted from the arc source point due to their high time resolution. In fact the arc fault location capability is very essential for the distribution management system and/or outage management system. However, determining the exact location of the power arcing fault on the field using wireless antennas is a challenging task, especially in multipath propagation environments. To address this problem, wideband signals are considered, since such signals can provide accurate range of measurement. In this article, the power arc position estimation is studied for wideband signal systems in conjunction with a performance analytical algorithm namely leading edge method. After a brief introduction of the use of wideband arc signals and their positioning applications, the leading edge detection method is investigated from a wideband arc signal perspective. Experiments of arc generation and radiation signal measurement are conducted and, using the measured electromagnetic data, the leading edge method is applied to the actual received waveforms captured by 4 antennas placed around the arc source point. In the process, the time of arrival and received signal strength from the actual waveforms are utilized to locate the arc radiation source point, and the results from the process are compared against the actual source location. It is observed that time-based leading edge positioning is well suited for wideband signals of the power arcing faults.*

Keywords: *power arc, radio frequency, electromagnetic radiation, antenna, signal arrival time, arc source location, signal processing, radio signal propagation, time delay estimation, radio measurement.*

Nomenclature

DF	Directional Finding
PA	Propagation Attenuation
RF	Radio Frequency
TDOA	Time Difference of Arrival
DDOA	Distance Difference of Arrival
DOA	Distance of Arrival
TOA	Time of Arrival
ASCC	Arc Source Cartesian Coordinates
LSM	Least Square Method
DMS	Distribution Management System
OMS	Outage Management System
FPA	First Peak of Arrival
LED	Leading Edge Detection
D_{ij}	Distance delay between antennas
d_{ij}	Distance difference of arrival
t_{ij}	Signal time difference of arrival
$n_x(t), n_y(t)$	Wide-sense Gaussian noise
c	Speed of signal wave (speed of light)
$s(t)$	RF-Signal
τ	Time delay
$F(X)$	Non-linear vector function
$X(x_i, y_i, z_i)$	Vector variable
ant_i	Antenna *i*
LEFAP	Leading Edge First Arrival Peak
DoA	Direction of Arrival
ATD	Arrival Time Difference
AoA	Angle of Arrival
LOS	Line of Sight
GPS	Global Positioning System
HF	High Frequency
VHF	Very High Frequency
VLF	Very Low Frequency
UHF	Ultra High Frequency
N_{ij}	Delay interval
N_i	Number of samples of antenna *i*
N_j	Number of samples of antenna *j*
N_s	Total number of samples
ρ_{P_T}	Power density of an electromagnetic wave
d	distance
P_R	Power received
P_T	Power transmitted
α	Signal amplitude attenuation factor

A	Signal propagation attenuation
ψ	Number of time difference of arrival
Ω	Ohm (impedance unit)

I. Introduction

This paper investigates fault location based on radio signals produced by arcing faults in power systems. Surveys have shown that the most common type of fault on power systems is the single phase to earth fault. Overhead line faults are 90 % predominantly of this kind, and 90 % of single phase to ground fault are arcing fault [**a**]. The air is the main insulation medium of overhead transmission lines. Therefore the fault path often contains an arc which bridges part of the air insulation gap when breakdown occurs. The arc in the line fault path is preceded by avalanche ionization at arc ignition and this causes non-linear current to circulate in the fault path. These non-linear currents occur at the frequencies in the Very Low Frequency (VLF) band up to the Ultra High Frequency (UHF) band, which causes any matched antenna like structures connected to or forming part of the current path to radiate electromagnetic fields.

The fact that arcing faults radiate electromagnetic waves calls for a new fault detection and location technology - monitoring and data logging of electromagnetic radiation events. This technique has many advantageous properties for an arcing fault detection and location system because their implementation in the power system is very cheap and easy to develop. Another advantage is that the technology does not require a direct connection to the power system, for exampleoverhead line under monitoring. However, the main advantage of using Very High Frequency (VHF) radiation as the basis for a distribution overhead line monitoring system is that the relatively low current levels of arcing faults on distribution networks can produce significant radiation in the VHF region of the electromagnetic spectrum. Further advantages are the relatively small reception antenna sizes could be adopted that will allow portability for experimentation purposes and the development of compact monitoring system equipment.

One of the main methods for time-difference evaluation is the cross-correlation of measured signals of different antennas**. [a]** Once an arcing fault has been detected at a monitoring station its location needs to be extracted from the electromagnetic waves radiation transient. This operation should be completed within few minutes; the calculations must therefore be relatively simple. In general, there are three location techniques that can be applied to radiation location problems: [**a**]

a. Arrival time difference (ATD or TDOA)
b. Direction finding (DF or AoA)
c. Propagation attenuation (PA)

These techniques and their potential application to the electromagnetic wave source location will be discussed in detail in next section.

This paper discusses in section II the power arc detection and location methods followed by the proposed leading edge detection theory in section III. The section IV deals with the description of the experiments and measurement data results, and, . subsequently, arc source location using measured data and the proposed method. Finally, in section V, the conclusions are presented with suggested improvements.

II. Power Arc Detection and Location Methods

Impulsive electromagnetic radiation can originate from many diverse sources in power system. The emission of radio wave energy in the form of power system electromagnetic waves as in lightning is related to the non-linear properties of the plasma arc. Since insulation is achieved via the natural air gap dielectric, it is therefore prone to flashover. This causes the majority of faults on the electricity supply system to occur on overhead lines. Power system arcing faults are induced by increasing the potential of the line above the insulation breakdown voltage for which the common causes are: (i) lightning, (ii) switching surges. They are also caused by a mechanical compromise of the insulation for which the common causes are: (iii) trees falling or growing up to the line, (iv) wind causing conductor clashing, (v) wind driven objects, (vi) broken or polluted insulators and (vii) ice causing conductor sagging or breakage.

II.1 Arrival Time Difference (ATD) techniques

There are several approaches of RF-signal based electromagnetic radiation source location. The location of the electromagnetic wave origin from the reception space requires the detection of the Line of Sight (LOS) of wave-front. [**a**] Clear reception of the LOS space waves will allow the extraction of accurate information that can be used for fault location. Problems caused by reflected and refracted space waves should be overcome by discriminating the direct space wave using wideband reception or digitization techniques. For a narrowband system, such problems could become more significant. However, since the LOS wave will always arrive before any wave from another path, its propagation distance can be extracted by using Arrival Time Difference (ATD) techniques. [**a**]

This method records the Time of Arrival (TOA) of the electromagnetic waves via LOS space wave at each of four antennas and calculates the location from the differences between the arrival times using hyperbolic equations. This technique has been successfully developed for the location of lighting induced electromagnetic waves, firstly using VLF band electromagnetic waves and more recently using VHF band electromagnetic waves. **[b]** If it is necessary to

locate arcs within a relatively small area such as a substation then all 4 ATD antennas can be combined and their data capturing synchronized within a single capture board. For greater coverage for geographically displaced monitoring sites, the Global Positioning System (GPS) can be used to provide accurate synchronization among the 4 monitoring stations . [**a**] The accuracy of the ATD location estimation is limited by the accuracy of the electromagnetic waves TOA information of the 4 monitoring antennas. [**a**]

II.2 Direction finding (DF)

Direction finding (DF) systems estimate the position location of a source by measuring the Direction of Arrival (DoA), or Angle of Arrival (AoA), of energy from the source as illustrated in Figure 1. [**a**] The DoA measurement restricts the location of the source to a line. Multiple DoA measurements from multiple sensors are used in a triangulation configuration to estimate the location of the source that lies on the intersection of such lines.

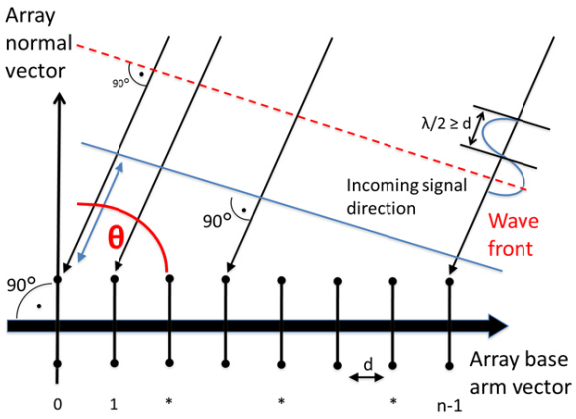

Figure 1. Direction or angle of arrival

While only two DoA estimates at minimum are required to estimate the position location of a source, multiple DoA estimates are commonly used to improve the estimation accuracy. [**a**] DoA estimation is performed by signal parameter estimation algorithms that exploit the phase differences or other signal characteristics between closely spaced antenna elements of an antenna array and employ phase-alignment methods such as beam/null steering. The spacing of elements within the antenna array is typically less than half a wavelength. This alignment is required to produce phase differences of the order of π radians or less, to avoid ambiguities in the DoA estimate. [**a**]

The resolution of DoA estimators improves as the baseline distances between the antennas increase. This improvement, however, is at the expense of ambiguities. As a result, DoA estimation methods are often used with short baselines to reduce or eliminate the ambiguities and long baselines to improve resolution [refs].

II.3 Propagation attenuation (PA)

In free space, all electromagnetic waves (radio, light, X-rays, etc.) obey the inverse-square law which states that the power density of an electromagnetic wave is proportional to the inverse of the square of the distance from a point source as:

$$\rho_{P_T} \propto \frac{1}{d^2} \qquad (1)$$

Doubling the distance from a transmitter means that the power density of the radiated wave at that new location is reduced to one-quarter of its previous value. The power density per surface unit is proportional to the product of the electric and magnetic field strengths. Thus, doubling the propagation path distance from the transmitter reduces each of their received field strengths over a free-space path by one-half as illustrated in Figure 2. {explain the figure, add axis label, and placement details}

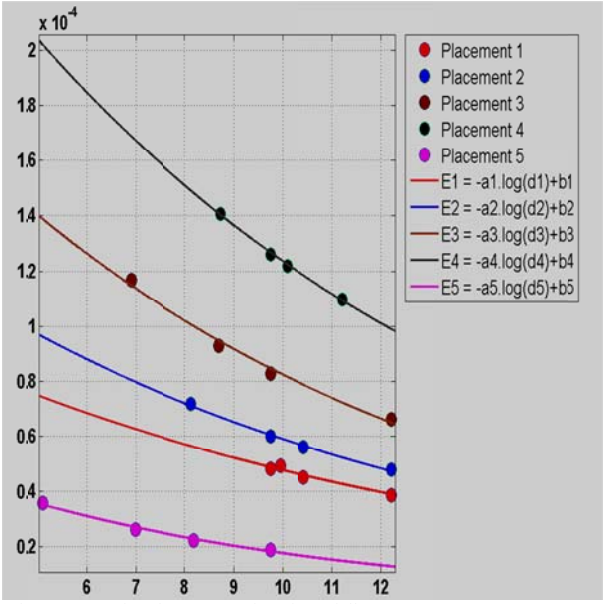

Figure 2. RF signal energy as function of distance

The signal propagation attenuation (*A*) is defined as the reduction in magnitude of a radio frequency signal from the transmitting station on passing along any transmission path. [**a**] It is directly proportional to the frequency and distance of transmission. The general formula is given as:

$$A = 10\log_{10}\frac{P_R}{P_T}, [dB] \qquad (2)$$

Where, P_R is the signal power received by the antenna in Watts, P_T signal power transmitted by the arcing fault in Watts. Below is a brief description of the

common features of the above mentioned RF-signal arrival-time based methods. In analytic geometry, the distance d between two points, (x_i, y_i) and (x_j, y_j), of the *xy*-plane is expressed as:

$$d = \sqrt{(x_i - y_i)^2 + (x_j - y_j)^2} \quad (3)$$

Similarly, given points (x_i, y_i, z_i) and (x_j, y_j, z_j) in three-space, the distance between them is:

$$d = \sqrt{(x_i - x_j)^2 + (y_i - y_j)^2 + (z_i - z_j)^2} \quad (4)$$

These formulas are easily derived by constructing a right triangle and applying the Pythagorean Theorem. Under this concept, with an antenna *i* located at (x_i, y_i, z_i), for example, the source location coordinate (x_s, y_s, z_s) can be expressed, using the speed of the RF signal *c*, which is the same as the light speed, and the RF signal arrival time at antenna *i*, t_i as follows: [**a**]

$$t_i * c = \sqrt{(x_s - x_i)^2 + (y_s - y_i)^2 + (z_s - z_i)^2} \quad (5)$$

Similar relationship to the above can be obtained from antennas for $i = 2 \ldots n$, where n is the total number of antennas placed. Using the above relationship in (1), an accurate estimate of the arcing source coordinate is determined from the measured times of arrival (TOA) and the coordinates of the antennas. [1]
In order to estimate the time delay or TOA, two antennas are needed to capture the transmitted signal $s(t)$. Assuming that the signal $y(t)$ is the replica of $x(t)$ captured by antenna ant_1 but being delayed by t_{12}. The signals$x(t)$ and$y(t)$received by a pair of antennas are separated by distance $d_{12} = c * t_{12}$, are expressed as: [1]

$$\begin{aligned} x(t) &= s(t) + n_x \\ y(t) &= \alpha s(t + \tau) + n_y(t) \end{aligned} \quad (6)$$

where α is the signal amplitude attenuation factor, n_x and $n_y(t)$are the wide-sense Gaussian noise processes which are uncorrelated with the signal of interest $s(t)$and τ is the time delay between the signal arrival time. Another way of locating a source using the same arrival time scheme is to draw a circle of radius corresponding the arrival distance for each antenna as illustrated in Figure 1. This way is useful especially when omnidirectional antennas are used. The arc source is determined as the intersection point of the distance of arrival (DOA) radii. [1] The common problem of the above mentioned arrival time based methods is that, due to the noisy RF signals measured at antenna, the exact arrival time point is not always straightforward. To solve the problem, we propose a method of arrival time approach for arc source location by using the Leading Edge first arrival peak (LEFAP) of the RF signals as to decide the arrival time.

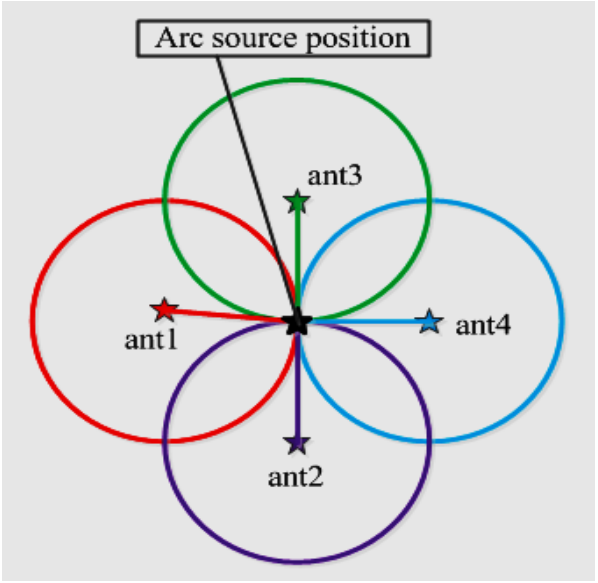

Figure 2.The source position placed at the intersection of the circles. The measured distances of arrival (DOA) are the radii of the circle centered at each antenna.

In the next section, the LEFAP method is introduced and discussed in details.

III. Leading Edge Detection Method

The definition of time of arrival (TOA) for position determination needs further explanation. The fundamentals of time of arrival (TOA) are based on measuring the propagation time that a signal takes to travel from the radiation source to an antenna. This time measurement is converted into distance by multiplying the speed of the signal in a medium to the TOA. The calculation of TOA, depends on the threshold point sets such that the LEFAP is above the noise level. In order to avoid under and/or over-estimating the threshold point, it needs to be set with good accuracy. Various threshold methods have already been developed by **[a]-[d].** The typical method is to choose the threshold at about 10 % of the signal rising time period. Such simple threshold strategy results in poor performance because in some cases the actual signal FPA is buried in the noise. A better strategy is to use a new proposed method which is to set the threshold point at least close to the half of the positive first peak amplitude of the expanded waveforms. If there is any displacement from the peak to the leading edge and it is common to all receivers, then this displacement can be arbitrarily chosen to suit

the algorithm, without any need to reference the peak. However, the proposed leading edge algorithm is based on estimating the position of the zero-crossing amplitude of the received signal by linearly projecting a point which crosses the threshold line for an antenna: , i.e. N_1 and N_2 respectively for antenna 1 and 2 .

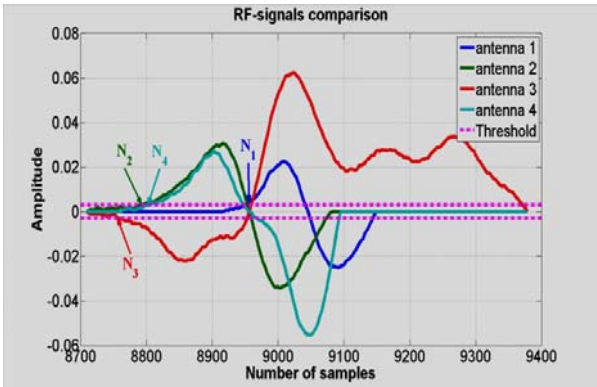

Figure 3. RF signal first peak time of arrival calculation using the leading edge detection method

The measured signal data based on the 5 different placements are used to calculate TOA, TDOA, DOA and DDOA and the results are presented respectively in Tables V, VI, VII and VIII. The algorithm used to derive these exact measured values based on the captured signal data is explained as follows: The antennas signal leading peak as illustrated in Figure 3 is measured using a signal window width which was obtained by quantizing and truncation of the actual signal samples in a rectangular window having a length L. The number of samples (N_s) contained in that window is determined by the interval $L_1 \leq M \leq L_2$, and the interval sequence duration is $L = L_2 - L_1 + 1$. The points N_1, N_2, N_3 and N_4 for the antennas 1, 2, 3 and 4 correspond to the point where their respective waveforms intersect the threshold line ($y = \gamma$), with γ being a constant value. The difference $N_i - N_j$ is the interval between antennas *i* and *j* and it is also known as sampling delay between antennas *i* and *j* which is used to calculate TDOA as $[(N_i - N_j)/N_s] \times T_s$. Similarly TOA is calculated as $[N_i/N_s] \times T_s$, where T_s is the sampling period. Assuming four antennas positioning systems, as illustrated in Figures 2 and 4, the total number (ψ) of the time differences of arrival (TDOA) is given by $\psi = n(n-1)/2$, where n is the number of antennas. In this experiment n = 4, thus gives $\psi = 6$, and the TDOA values are as follows: t_{12}, t_{13}, t_{14}, t_{23}, t_{24}, and t_{34}. Having calculated TOA and TDOA, the distances of arrival (DOA) and the difference distances of arrival DDOA are directly derived as DOA = c×TOA and DDOA = c×TDOA where c is the speed of signal propagation (similar to the speed of light). Finally, using these TDOA values, the arc source Cartesian coordinates are finally calculated by solving (1) and Newton–Raphson nonlinear iteration technique procedure according to [1]-[2]. An experimental method of obtaining the needed arrival times (TOA) or the time difference of arrival (TDOA) and the feasibility study of the method proposed using the acquired arrival times are the main subject of the next section.

IV. Arc Location Experiment and Results

In order to evaluate the performance of the proposed method, we performed a set of arc location experiments as shown in Figure 2 and Figure 4. As shown in Figure 4 only 2 types of topologies (horizontally and vertically) for the antennas' placements are made. These two topologies will help to choose the suitable antennas arrangement that could be adopted for power arc fault detection in power distribution network. [1]

IV.1 Experiment set-up

The set-up depicted in Figure 2 consists of four antennas placed around the arc source covering a portion of RF radiation space. The distances between two neighboring antennas vary in interval of 2 to 12 m. The antennas used as shown in Figure 3 are Yagi – Uda antennas which cover a frequency range of 47 - 862 MHz with 75 Ω impedance. The Yagi – Uda antenna is commonly known as a Yagi antenna that is a directional antenna consisting of a driven element namely a dipole or folded dipole and additional parasitic elements such as reflector and directors. The reflector element is slightly longer typically at about 5% longer than the driven dipole, whereas the so-called directors are a little shorter. Yagi-Uda antennas are directional along the axis perpendicular to the dipole in the plane of the elements, from the reflector toward the driven element and the director(s). Highly directional antennas such as the Yagi-Uda are commonly referred to as beam antennas due to their high gain. However, the Yagi-Uda design only achieves this high gain over a rather narrow bandwidth, making it useful for specific analytical communications bands like high frequency (HF), very high frequency (VHF), and ultra-high frequency (UHF) bands; therefore it is appropriate to be used in the measurements of this current experiment. The arc is produced by a pine tree leaning on an iron rod at a gap length of 5 mm, which is located at (0.07, 8.89, 5.1) measured in meter in the Euclidian plan, away from the closest antenna (used as a reference antenna) and that is the antenna 3 in placement 1, antenna 4 in placement 2, antenna 4 in placement 3, antenna 2 in placement 4 and antenna 1 in placement 5. A high voltage AC source (voltage generator 0~260 V) feeding a transformer of 20/0.4 kV is used to generate the arcs. The Figure 2 shows the actual arc produced between the current conductor and a pine tree during the experiment carried out in the high voltage laboratory at Aalto University of Finland. The measurement room size is 21 m × 15 m ×

15 m, and the antennas are placed at about 10 m from the wall surface and 12 m from the ceiling thus the signal reflections are avoided for the FPA of signals integrity. The antennas input is connected through coaxial cable of 3 m to a multi-channel LeCroy digitizer of 2 GHz/s sampling frequency in order to capture the radiated RF signals from the arcs. The pine tree roots are placed in a bowl filled with water in order to maintain the tree into its natural environment conditions. The tree's total length is 9 m and leaning on the metallic rod at about 5.1 m from the floor. The tree has a diameter of 75 mm at its bottom and 58 mm at the point where the arc is produced. The arc current and voltage across the tree is measured and recorded. Having obtained the current and a voltage value, the tree's resistance is determined at about 316 kΩ. For each channel, signals are captured at the sample rate of 20000 samples per microsecond and illustrated in Figure 5.

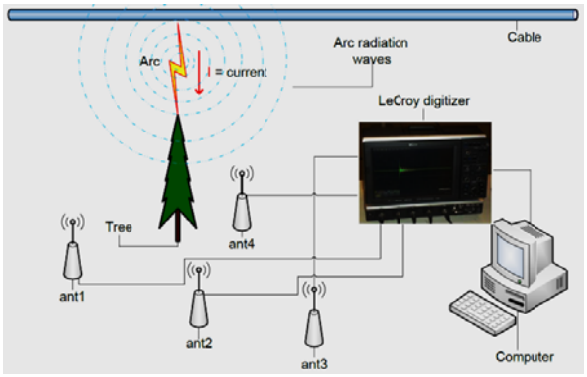

Figure 4. The experimental setup for arc generation, a high voltage AC source of 20 kV is used to generate the arcs. The arc is produced by tree leaning on an iron rod.

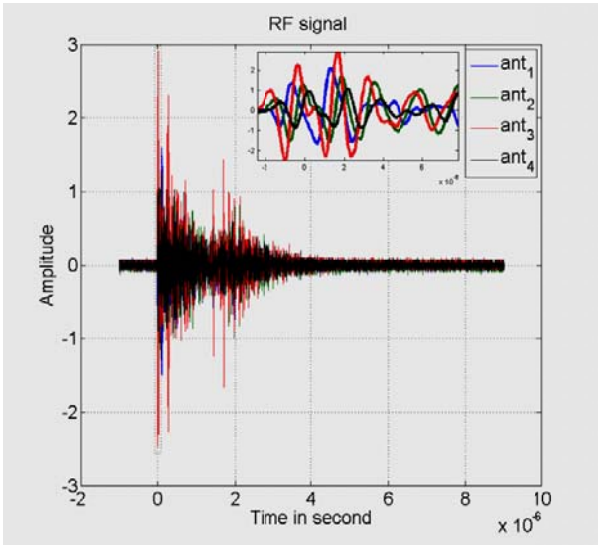

Figure 5. The captured arc RF signal in placement 1

TABLE II
ARC SOURCE POSITION

Placement	ant_1			ant_2		
	x	*y*	*z*	*x*	*y*	*z*
1	-7.35	0	1.1	-3.68	0	1.1
2	-7.35	0	1.1	-3.68	0	1.1
3	-7.35	0	1.1	-3.68	2.1	1.1
4	-5.53	0	1.1	-3.76	2.1	1.1
5	0	5.71	1.1	0	3.16	1.1
Placement	ant_3			ant_4		
	x	*y*	*z*	*x*	*y*	*z*
1	0	0	1.1	2	0	1.1
2	0	0	1.1	2	2.1	1.1
3	0	0	1.1	2	3.63	1.1
4	-2.6	0	1.1	0	0	1.1
5	0	1.74	1.1	0	0	1.1

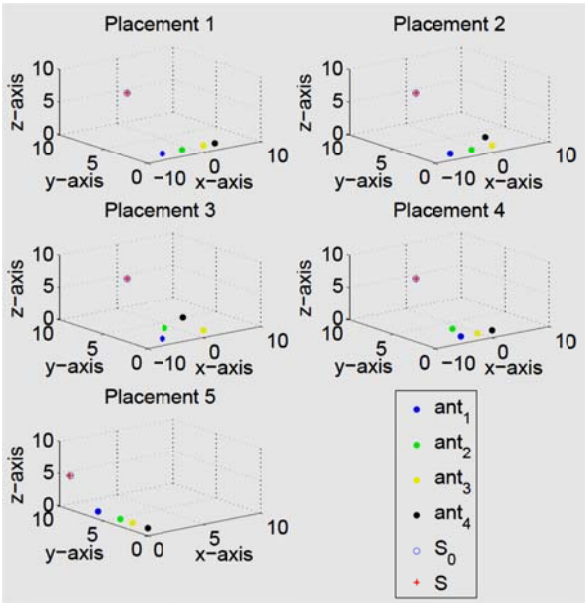

Figure 6. Antennas placements [1]

As shown in Figure 4 and Table II the five placement methodologies are done as follow:

i. Placement 1: the antennas are horizontally placed on the *x*-axis.
ii. Placement 2: antennas 1, 2 and 3 are horizontally placed on *x*-axis and the antenna 4 is slightly shifted toward to the arc source.
iii. Placement 3: the antennas 1 and 3 remain on the on *x*-axis while antennas 2 and 4 are placed much closer to the arc source: Placement 4: the antennas 1, 3 and 4 are

horizontally placed on *x*-axis and the antenna 2 is moved forward and closer to the arc source point.

iv. Placement 5: The 4 antennas are all vertically placed on *y*-axis.

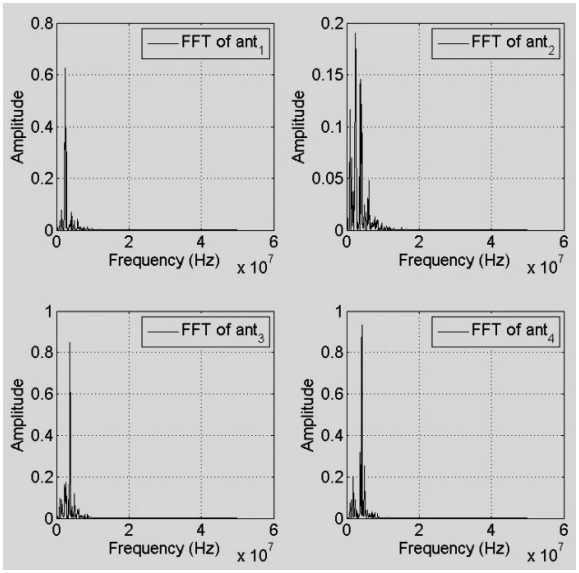

Figure 7. FFT of the captured arc RF signal in placement 1

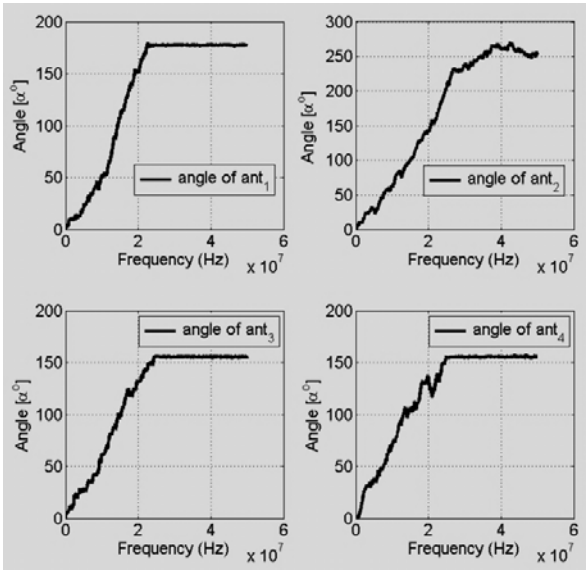

Figure 8. Phase angle of the captured arc RF signal in placement 1

From these 5 placements the recorded arc signal waveforms are plotted as shown in Figure 5. In figure 5, the signal variation is observed with time. However, we have no any idea about this signal by the time record. By the Fast Fourier transform (FFT) expressed in (7) the signals of interest are located between 10 MHz and 40 MHz mixed with other noises as illustrated in Figure 7.

$$F(\omega) = \frac{2}{T}\int_{-T/2}^{T/2} s(t)e^{-ik\omega t}\,dt \quad (7)$$

where $\omega = 2\pi f$ with the frequency $f[Hz] = 1/T$ and $T[s]$ the observation time period, $k = 2\pi/\lambda$ is the wave number while $\lambda[m]$ is the signal $s(t)$ wavelength. The time signal squared $[s(t)]^2$ represents the energy contained in the signal distributes over time *t*, while its amplitude or spectrum squared $|F(\omega)|^2$ represents the energy distributes over frequency (therefore the term power density spectrum). Obviously, the same amount of energy is contained in either time or frequency domain, as indicated by Parseval's formula as:

$$E = \int_{-\infty}^{+\infty} |s(t)|^2 \mathrm{dt} = \int_{-\infty}^{+\infty} |F(\omega)|^2\, d\omega \quad (8)$$

Similarly from the FFT computation, the variation of the signal phase angle ($\alpha[.^0]$) in frequency domain is also calculated and plotted in Figure 8.

IV.2 Results

In this section the TOA, TDOA and the ASCC are calculated and compared with their corresponding actual values. In Figure 4-8, ant_1 (with $i = 1, 2, 3, \ldots 4$) stands for antenna. From the arrangement of the antennas, and under the assumption that the arc RF signals travel at the speed of light, the theoretical RF signal arrival times (TOA) in placement 1, are calculated using (5). From $t = 0$ of arc onset, in antenna j (with $j = 1, 2, 3, \ldots 4$), TOA in placement 1 is found as follows: $t_1 = 40.716\,ns$, $t_2 = 34.745\,ns$, $t_3 = 32495\,ns$ and $t_4 = 33.165\,ns$. Similarly the rest of the theoretical TOA in other placement are calculated and the results are presented in Table I. Next the signal times differences of arrival (TDOA) between pairs of antennas are derived by taking the algebraic subtraction between pair of TOA as illustrated in Table II. From the results in Tables II, the actual distance differences of arrival (DDOA) which are the signal propagation distances between pairs of antennas are calculated and presented in Table IV.

TABLE I
ACTUAL TIME OF ARRIVAL TOA [ns]

Placement	t_1	t_2	t_3	t_4
1	40.716	34.745	32.495	33.165
2	40.712	34.742	32.495	27.095
3	40.710	29.002	32.495	23.007
4	37.371	29.116	33.637	32.495

5	17.033	23.293	27.309	32.495

TABLE II
ACTUAL TIME DIFFERENCE OF ARRIVAL BETWEEN THE ANTENNAS (TDOA) [ns]

Placement	t_{12}	t_{13}	t_{13}	t_{23}	t_{24}	t_{34}
	5.963	8.201	7.524	2.238	1.561	0.677
2	5.963	8.201	13.594	2.238	7.632	5.393
3	11.704	8.201	17.682	3.503	5.978	9.481
4	8.254	3.728	4.864	4.525	3.389	1.136
5	6.260	10.276	15.461	4.016	9.201	5.185

TABLE III
ACTUAL DISTANCE OF ARRIVAL (DOA) [m]

Placement	d_1	d_2	d_3	d_4
1	12.215	10.424	9.748	9.949
2	12.214	10.423	9.748	8.128
3	12.213	8.700	9.748	6.902
4	11.211	8.735	10.09	9.748
5	5.110	6.988	8.193	9.748

TABLE IV
ACTUAL DISTANCE OF ARRIVAL (DDOA) [m]

Placement	d_{12}	d_{13}	d_{13}	d_{23}	d_{24}	d_{34}
1	1.791	2.467	2.266	0.675	0.474	0.201
2	1.791	2.465	4.085	0.674	2.294	1.620
3	3.513	2.465	5.311	1.048	1.798	2.846
4	2.477	1.120	1.463	1.356	1.014	0.343
5	1.878	3.083	4.638	1.205	2.760	1.556

TABLE V
MEASERED TIME OF ARRIVAL TOA [ns]

Placement	t_1	t_2	t_3	t_4
1	41,778	34,704	31,735	33,060
2	37,880	33,439	30,059	30,883
3	37,257	28,699	32,512	25,385
4	36,969	29,717	35,536	30,917
5	19,445	22,690	22,782	24,369

TABLE VI
MEASURED TIME DIFFERENCE OF ARRIVAL BETWEEN THE ANTENNAS (TDOA) [ns]

Placement	t_{12}	t_{13}	t_{14}	t_{23}	t_{24}	t_{34}
1	7,074	10,043	8,717	2,969	1,644	1,325
2	4,442	7,821	6,998	3,379	2,556	0,823
3	8,558	4,745	11,872	3,813	3,314	7,127
4	7,252	1,433	6,051	5,819	1,201	4,618
5	3,246	3,337	4,924	0,091	1,679	1,587

TABLE VII
MEASURED DISTANCE OF ARRIVAL (DOA) [m]

Placement	d_1	d_2	d_3	d_4
1	12,533	10,411	9,521	9,918
2	11,364	10,032	9,018	9,265
3	11,177	8,610	9,754	7,615
4	11,091	8,915	10,661	9,275
5	5,833	6,807	6,834	7,311

TABLE VIII
MEASURED DISTANCE OF ARRIVAL (DDOA) [m]

Placement	d_{12}	d_{13}	d_{14}	d_{23}	d_{24}	d_{34}
1	2,122	3,013	2,615	0,891	0,493	0,398
2	1,333	2,346	2,099	1,014	0,767	0,247
3	2,567	1,423	3,562	1,144	0,994	2,138
4	2,176	0,430	1,815	1,746	0,360	1,386
5	0,974	1,001	1,477	0,027	0,504	0,476

According to [1] the solution of (9) is formed by an application of the Newton–Raphson technique procedure to solve the nonlinear function $F(X) = 0$. The equation (2) is a reformulation of (1) thus yields to a nonlinear function vector $F(X)$ in order to be solved with numerical methods namely a least square method (LSM).

$$F(X) = \sqrt{(x_s - x_i)^2 + (y_s - y_i)^2 + (z_s - z_i)^2} - d_{ij} (9)$$

where $F(X)$ is a non-linear vector function discussed in detail by [1] and $X = (x, y, z)$is a vector variable. Function $F(X)$ is expanded using Taylor's series in vicinity of the root iteration $X^0 = (x^0, y^0, z^0)$ as the iteration guess point. Finally as illustrated Table X the arc source $(xyz) -$ coordinates (ASCC) per placement is computed and compared with the actual ASCC as shown in Table XI and Figures 9 and 10. The error between the actual and the measured ASCC as seen in Figure 9 oscillates from 0.0067 up to 0.85, which is acceptable. However placement 1 offers better detection solution followed respectively by placements 4, 3, 2 and 5. Since the error per placement is less than 10%, it implies that the method of using the leading edge peak of the signal shows very good accuracy which is also scientifically meaningful. The good performance of the proposed method in this experiment is confirmed by Figure 10, where it is observed that the measured ASCC per placement lies inside a sphere of 1 m radius centered at the actual source coordinates namely S_o and marked with a red filled circle (○). The measured sources are follows: S_1, S_2, S_3, S_4 and S_5 and they are respectively marked with dark blue, green, black, purple and light blue filled circle (○).

TABLE X
ARC SOURCE POSITION

Placement	Actual source			Measured source		
	x	*y*	*z*	*x*	*y*	*z*
1	0.0696	8.8771	5.0942	0.0772	8.9060	5.1072
2	0.0696	8.8771	5.0942	-0.002	8.6207	4.9712
3	0.0696	8.8771	5.0942	0.0095	8.6869	4.9911
4	0.0696	8.8771	5.0942	0.0799	8.9090	5.1091
5	0.0696	8.8771	5.0942	0.0629	8.0265	4.5462

TABLE XI
ERROR IN ASCC

Placement	*x*	*y*	*z*
1	0.0076	0.0289	0.013
2	0.0676	0.2564	0.123
3	0.0601	0.1902	0.1031
4	0.0103	0.0319	0.0149
5	0.0067	0.8506	0.548

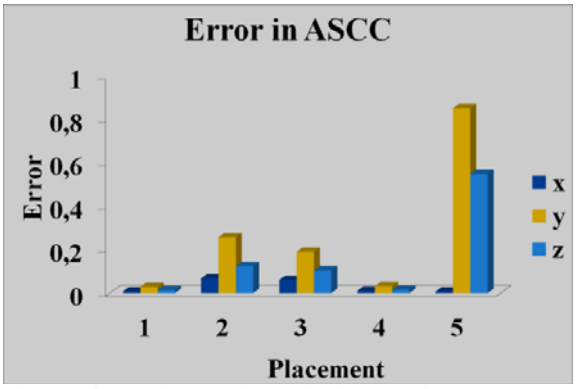

Figure 9. The error between the actual and measured ASCC

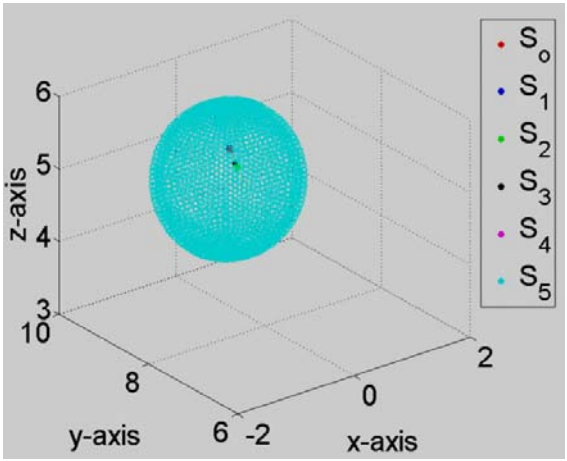

Figure 10. Measured and actual ASCC in 3D Cartesian plane

IV.1 discussion

The placements 3 and 4 which are almost located at the same distance (see Figure 11) from the actual arc source point i.e. in placement 1 produce similar energy intensity as illustrated in Figure 12. Thus confirms as well the similarity of their respective error margin as shown in Figure 9. Their detection and location solution is as expected since the antennas used in this experiment are all identical. From a deep observation of Figures 11 and 12, it can be seen that the distance and the energy are inversely proportional as previously defined in (1). The antennas the antenna 3 that is close to the arc source point and also used as reference point presents much higher energy compared to the others as expected. The errors as shown in Table XI, also discussed by [1] come mainly from the signal reflection due the placement of antennas quite close to each other. However these errors seemed not to influence the signal integrity and measurement, since they are quite smalls thus the arc source fault when it occurs on the field can immediately be discovered because it will always lie within a unit circle when this proposed algorithm is used. However, from the experiment and initial analysis, the outcomes are (i) the new proposed method of time difference, using the signal LEFAP works at a reasonable level of accuracy and (ii) this new proposed algorithm of timing the LEFAP shows its potential in clarifying the arrival time point. Also, clear is that we need more tests with longer distance of the antenna placement from the arc source in locations on random selection.

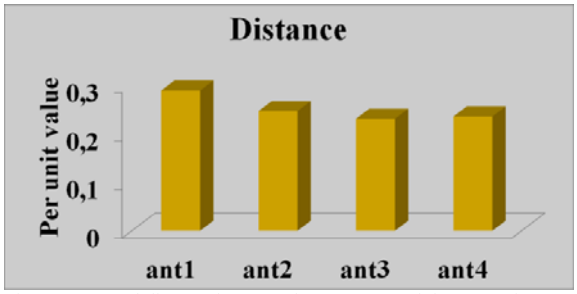

Figure 11 Actual distance between the antennas and the source in placement 1

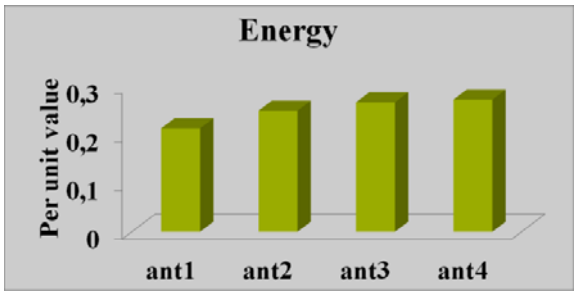

Figure 12 RF radiated energy captured by the antennas in placement 1

V Conclusion

This paper reported an experimental investigation of power arc source location using radio frequency measurements. The RF signal LEFAP method was applied on the captured arcing fault RF signals data by 4 antennas strategically placed around the actual arc source point, to determine the distance and time of arrival between these antennas and the actual power

arcing source point. It was observed that this new proposed arcing fault detection and location method shows its potential in clarifying the location technique at a reasonable level of accuracy. The measurement system accuracy in this experiment, which was an essential element in locating this type of arc signal source, was achieved as expected. The investigation found that this new method of signal LEFAP could be a very good and important detection and location tool that could be integrated to the distribution management system (DMS) and/or outage Management system (OMS) for accurate location of fault arcs, faster power supply restoration and minimized outage hours. Also, the investigation found that more tests were needed with longer distance of the antenna placement from the arc source in locations on random selection.

Acknowledgements

The authors gratefully acknowledge the contributions of TatuNieminen and Joni Klüss, for their work on building the laboratory experiment.

References

[1] ZokoBle, F; Lehtonen, M; Sihvola, A; Kim, C; "*Cross-Correlation Method for Power Arcing Source Monitoring System*",International Review of Electrical Engineering (IREE), onVol 9, No 2 (2014); p 440-452.

[2] Bartlett, E.J.; Moore, P.J.; "*Remote sensing of power system arcing faults*", Advances in Power System Control, Operation and Management, 2000. APSCOM-00. 2000 International Conference on Vol. 1 , 2000, pp. 49–53.

[3] Moore, P.J.; Portugues, I.E.; Glover, I.A.; "*Radiometric location of partial discharge sources on energized high-Voltage plant*", Power Delivery, IEEE Transactions on Vol. 20, 2005, pp. 2264-2272.

[4] Shihab, S.; Wong, K.L.; *"Detection of faulty components on power lines using radio frequency signatures and signal processing techniques"*, Power Engineering Society Winter Meeting, 2000. IEEE Vol. 4, 2000, pp. 2449–2452.

[5] Young, D.P.; Keller, C.M.; Bliss, D.W.; Forsythe, K.W.*; "Ultra-wideband (UWB) transmitter location using time difference of arrival (TDOA) techniques"*, Signals, Systems and Computers, 2003. Conference Record of the Thirty-Seventh Asilomar Conference on Vol. 2 , 2003, pp. 1225–1229.

[6] Sun, Y.; Stewart, B.G.; Kemp, I.J.*; "Alternative cross-correlation techniques for location estimation of PD from RF signal"*, Universities Power Engineering Conference, 2004. UPEC 2004. 39th International Vol. 1, 2004, pp. 143–148.

[7] ChyeHuat Peck; Moore, P.J.; *"A direction-finding technique for wide-band impulsive noise source"*, Electromagnetic Compatibility, IEEE Transactions on Vol. 43, 2001, pp. 149–1544.

[8] Yang, L.; Judd, M.D.; Bennoch, C.J.*; "Time delay estimation for UHF signals in PD location of transformers [power transformers]"*, Electrical Insulation and Dielectric Phenomena, 2004. CEIDP '04. 2004 Annual Report Conference, 2004, pp. 414-417.

[9] Azaria, M.; Hertz, D.; *"IEEE Transactions on Acoustics, Speech, and Signal Processing"*, Vol. 32, 1984, pp. 280-285.

[10] Soeta, Y.; Uetani, S.; Ando, Y.; *"Autocorrelation and cross-correlation analyses of alpha waves in relation to subjective preference of a flickering light"*, Engineering in Medicine and Biology Society, 2001. Proceedings of the 23rd Annual International Conference of the IEEE Vol. 1, 2001, pp. 635– 638.

[11] Alavi, B.; Pahlavan, K.; *"Modeling of the TOA-based distance measurement error using UWB indoor radio measurements"*, Communications Letters, IEEE Vol. 10, 2006, pp. 275–277.

[12] Mallat, Achraf; Louveaux, J.; Vandendorpe, L.; *"UWB based positioning: Cramer Rao bound for Angle of Arrival and comparison with Time of Arrival"*, 2006 Symposium on Communications and Vehicular Technology, pp. 65–68.

[13] Alsindi, N.; Xinrong Li; Pahlavan, K.; *"Analysis of Time of Arrival Estimation Using Wideband Measurements of Indoor Radio Propagations"*,Instrumentation and Measurement, IEEE Transactions on Vol. 56, 2007, pp. 1537-1545.

[14] Rohrig, C.,Kunemund, F., *"Mobile Robot Localization using WLAN Signal Strengths"*.Intelligent Data Acquisition and Advanced Computing Systems: Technology and Applications, 2007. IDAACS 2007. 4th IEEE Workshop, pp. 704 - 709

[15] Bo-ChiehLiu,Ken-Huang Lin *"Accuracy Improvement of SSSD Circular Positioning in Cellular Networks"*.Vehicular Technology, IEEE Transaction, pp. 1766 - 1774

[16] Motter, P. , Allgayer, R.S. ; Muller, I. ; Pereira, C.E. ; Pignaton de Freitas, E. *"Practical issues in Wireless Sensor Network localization systems using received signal strength indication"*.Sensors Applications Symposium (SAS), 2011 IEEE, pp. 227 - 232

[17] Chih-Chun Lin, She-Shang Xue; Yao, L. *"Position Calculating and Path Tracking of Three Dimensional Location System Based on Different Wave Velocities"*.Dependable, Autonomic and Secure Computing, 2009. DASC '09. Eighth IEEE International Conference, pp. 436 - 441

[18] El Arja, H., Huyart, B.; Begaud, X. *"Joint TOA/DOA measurements for UWB indoor propagation channel using MUSIC algorithm"*.Wireless Technology Conference, 2009, pp. 124 - 127

[19] Born, A.,Schwiede, M. ; Bill, R. *"On distance estimation based on radio propagation models and outlier detection for indoor localization in Wireless GeosensorNetworks"*,Indoor Positioning and Indoor Navigation (IPIN), International Conference 2010, pp. 1 - 6

[20] Fugen Su, WeizhengRen; Hongli Jin, *"Localization Algorithm Based on Difference Estimation for Wireless Sensor Networks"*.Communication Software and Networks. ICCSN '09. International Conference, 2009, pp. 499 - 503

[21] Bing-Fei Wu , Cheng-Lung Jen ; Kuei-Chung Chang, *"Neural fuzzy based indoor localization by Kalman filtering with propagation channel modeling"*. Systems, Man and Cybernetics. ISIC. IEEE International Conference, 2007, pp. 812 - 817

[22] Benkic, K., Malajner, M.; Planinsic, P.; Cucej, Z. *"Using RSSI value for distance estimation in wireless sensor networks based on ZigBee"*.Systems, Signals and Image Processing, 2008. 15th International Conference, 2008, pp. 303 - 306

[23] Suk-Un Yoon, Liang Cheng; Ghazanfari, E.; Pamukcu, S.; Suleiman, M.T. *"A Radio Propagation Model for Wireless Underground Sensor Networks"*.Global Telecommunications Conference (GLOBECOM 2011), 2011, pp. 1 – 5

Authors' information

Frank Zoko Ble obtained a B.Sc. in Physics in Ivory coast National University, Abidjan in 1997. He received M.Sc. in Electrical Engineering in Helsinki University of Technology (TKK), Espoo, Finland in 2010. He is a planning and design engineer for the City of Espoo, the central state-owned

enterprise, Finland.Also, he is working toward his PhD degree in Aalto University, School of Electrical Engineering. His research interests are in electric power arcs detection using radio frequency measurements. He is a researcher in the Department of Electrical of Aalto University, School of Electrical Engineering, Finland.

Matti Lehtonen (1959) was with VTT Energy, Espoo, Finland from 19987 to 2003, and since 1999 has been a professor at the Helsinki University of Technology (TKK), where he is now head of Electrical Engineering department. MattiLehtonen received both his Master's and Licentiate degrees in Electrical Engineering from Helsinki University of Technology , in 1984 and 1989 respectively, and the Doctor of Technology degree from Tampere University of technology in 1992. The main activities of Professor Lehtonen include power system planning and asset management, power system protection including earth fault problems, harmonic related issues and applications of information technology in distribution systems. He is a Professor in Aalto University, School of Electrical Engineering, Finland.

Charles Kim received a PhD degree in electrical engineering from Texas A&M University (College Station, TX) in 1989. Since 1999, he has been with the Department of Electrical and Computer Engineering at Howard University. Previously, Dr. Kim held teaching and research positions at Texas A&M University and the University of Suwon. Dr. Kim's research includes failure detection, anticipation, and system safety analysis in safety critical systems in energy, aerospace, and nuclear industries. Several inventions of his in the research area have been patent field through the university's intellectual property office. Dr. Kim is a senior member of IEEE and the chair of an IEEE chapter in Washington Baltimore section.

Ari Sihvola was born on October 6th, 1957, in Valkeala, Finland. He received the degrees of Diploma Engineer in 1981, Licentiate of Technology in 1984, and Doctor of Technology in 1987, all in Electrical Engineering, from the Helsinki University of Technology (TKK), Finland. Besides working for TKK and the Academy of Finland, he was visiting engineer in the Research Laboratory of Electronics of the Massachusetts Institute of Technology, Cambridge, in 1985–1986, and in 1990–1991, he worked as a visiting scientist at the Pennsylvania State University, State College. In 1996, he was visiting scientist at the Lund University, Sweden, and for the academic year 2000–01 he was visiting professor at the Electromagnetic and Acoustics Laboratory of the Swiss Federal Institute of Technology, Lausanne. In the summer of 2008, he was visiting professor at the University of Paris XI, France. Ari Sihvola is professor of electromagnetic in Aalto University School of Electrical Engineering (former name before 2010: Helsinki University of Technology) with interest in electromagnetic theory, complex media, materials modeling, remote sensing, and radar applications. He is Chairman of the Finnish National Committee of URSI (International Union of Radio Science) and Fellow of IEEE. He also served as the Secretary of the 22nd European Microwave Conference, held in August 1992, in Espoo, Finland. He was awarded the ve-year Finnish Academy Professor position starting August 2005. He is also director of the Finnish Graduate School of Electronics, Telecommunications, and Automation (GETA).